ELSEVIER

www.elsevier.nl/locate/carres

Carbohydrate Research 324 (2000) 17–29

CARBOHYDRATE RESEARCH

Bivalency and epitope specificity of a high-affinity IgG3 monoclonal antibody to the *Streptococcus* Group A carbohydrate antigen. Molecular modeling of a Fv fragment

J. Bruce Pitner [a], Wayne F. Beyer [a], Thomas M. Venetta [a], Colleen Nycz [a], Michael J. Mitchell [a], Shannon L. Harris [b], Jose R. Mariño-Albernas [b], France-Isabelle Auzanneau [b], Farzin Forooghian [b], B. Mario Pinto [b,*]

[a] *Becton Dickinson Research Center, PO Box 12016, Research Triangle Park, NC 27709, USA*
[b] *Department of Chemistry and Institute of Molecular Biology and Biochemistry, Simon Fraser University, Burnaby, BC, Canada V5A 1S6*

Received 7 July 1999; accepted 24 September 1999

Abstract

The binding of Strep 9, a mouse monoclonal antibody (mAb) of the IgG3 subclass directed against the cell-wall polysaccharide of Group A *Streptococcus* (GAS), has been characterized. The intact antibody and proteolytic fragments of Strep 9 bind differently to GAS: the intact mAb and F(ab)$'_2$ have greater affinity for the carbohydrate epitope than the monomeric Fab or F(ab)′. A mode of binding in which Strep 9 binds bivalently to portions of the polysaccharide on adjacent chains on GAS is proposed. A competitive ELISA protocol using a panel of carbohydrate inhibitors shows that the branched trisaccharide, β-D-Glc*p*NAc-(1→3)-[α-L-Rha*p*-(1→2)]-α-L-Rha*p*, and an extended surface are key components of the epitope recognized by Strep 9. Microcalorimetry measurements with the mAb and two synthetic haptens, a tetrasaccharide and a hexasaccharide, show enthalpy–entropy compensation as seen in other oligosaccharide–protein interactions. Molecular modeling of the antibody variable region by homology modeling techniques indicates a groove-shaped combining site that can readily accommodate extended surfaces. Visual docking of an oligosaccharide corresponding to the cell-wall polysaccharide into the site provides a putative model for the complex, in which a heptasaccharide unit occupies the site and the Glc*p*NAc residues of two adjacent branched trisaccharide units occupy binding pockets within the groove-shaped binding site.

Keywords: IgG3 monoclonal antibody; Group A *Streptococcus* polysaccharide; Epitope specificity; Multivalent interactions; Homology modeling

Abbreviations: AP, alkaline phosphatase; BSA, bovine serum albumin; CWPS, cell-wall polysaccharide; DTT, dithiothreitol; EDTA, ethylenediaminetetraacetic acid, disodium salt; ELISA, enzyme-linked immunosorbent assay; Fab, antigen-binding region of antibody; F(ab)$_2$, dimeric fragment containing both antigen-binding regions; F(ab)′, monomeric antigen-binding fragment that results from further digestion of F(ab′)$_2$; Fc, crystallizable fragment of antibody; Fv, variable region of antibody; FPLC, fast protein liquid chromatography; GAS, Group A *Streptococcus*; Glc*p*NAc, *N*-acetylglucosamine; HRP, horseradish peroxidase; Ig, immunoglobulin; mAb, monoclonal antibody; NPP, *p*-nitrophenyl phosphate; OPD, *o*-phenylenediamine; PAGE, polyacrylamide gel electrophoresis; PBS, phosphate buffered saline; RIA, radioimmunoassay; SDS, sodium dodecyl sulfate; TBS, tris buffered saline; Tris, tris(hydroxymethyl)aminomethane.

* Corresponding author. Tel.: +1-604-291-4327; fax: +1-604-291-3765.
E-mail address: bpinto@sfu.ca (B. Mario Pinto)

0008-6215/00/$ - see front matter
PII: S0008-6215(99)00279-7

1. Introduction

The Gram-positive Group A *Streptococcus* (GAS) are a widespread genus of bacteria that are pathogenic in humans. They are a primary cause of pharyngitis in humans and have been implicated in the development of the more serious condition of rheumatic fever and other diseases such as heart valve disease, glomerulonephritis, and rheumatoid arthritis [1–3]. Cross-reactivity between GAS carbohydrate antigens and tissue antigens has been suggested in the pathogenesis of these disease states [4–7]. Well-defined antibodies directed against carbohydrate epitopes could be used to clarify and to provide a molecular basis for the correlations. Furthermore, these antibodies could have use as improved immunodiagnostic reagents for the early detection of GAS infections. These applications require a more detailed understanding of the nature of intermolecular recognition between the cell-wall polysaccharide (CWPS) and monoclonal antibodies (mAbs) directed against this target. The structure of the CWPS has been shown to consist of a poly(L-rhamnopyranosyl) backbone composed of alternating α-L-(1→2) and α-L-(1→3) linkages that bear branching *N*-acetyl-β-D-glucopyranosylamine residues at alternate 3-positions [8–10]. In this paper, we report a comprehensive study to characterize the binding of Strep 9, a high-affinity mouse mAb directed against the CWPS of GAS.

2. Results

Strep 9 is a murine IgG3 Ab. This subclass of antibody is known to possess aberrant solubility characteristics depending upon the protein concentration, pH, and ionic strength. Attempts to purify Strep 9 using Protein-A affinity chromatography produced variable results depending upon the commercial source of the purification system. For instance, the Pharmacia mAb Trap Kit resulted in very low yields due to precipitation of Strep 9 upon neutralization of the acidic eluent from the column (data not shown). The precipitate could not be re-solubilized using various buffers, ionic strengths, or other additives.

The use of the Glc*p*NAc–agarose matrix produced a 40–50% increase in the overall yield of Strep 9, compared with the Protein-A matrix. The direct purification of Strep 9 from ascites avoids any changes in pH or ionic strength that can affect the solubility of the IgG3 mAb. Furthermore, purification on the Glc*p*NAc–agarose column selectively purifies correctly folded mAb from denatured mAb. Protein-A purification would not achieve this discrimination since the affinity is for the constant region rather than the antigen binding site.

The IgG3 subclass of murine mAbs is remarkably sensitive to papain digestion. Initial attempts to obtain Fab from Strep 9 consistently resulted in over-digestion of the protein. The parameters affecting digestion include the following: enzyme–substrate ratio, pH, protein concentration, digestion time, reductant concentration, chelator concentration and reaction temperature. These were optimized for an efficient digestion, as shown by the quantitative disappearance of the heavy chain and minor accumulation of low-molecular-weight peptides on SDS gels. The conditions required were much milder and used shorter reaction times than those used for other antibodies such as IgG2bs [11].

The Glc*p*NAc–agarose column used to purify Strep 9 from ascites and to purify Fab from undigested mAb was also used to investigate the relative affinities of the mAb and all the fragments generated by the enzyme digestion (see Fig. 1). In these experiments, the antibody or fragment was applied to the column and a linear gradient of Glc*p*NAc was used to elute any protein that remained bound after extensive washing with TBS. Both $F(ab)'_2$ and the parent mAb bound to the Glc*p*NAc column with approximately equal affinity and were eluted as sharp bands with the Glc*p*NAc gradient (Fig. 2). The Fab and F(ab)′ failed to bind appreciably.

The avidity of Strep 9 for immobilized heat-killed GAS was determined by both ELISA and RIA protocols. The value for the avidity was taken to be the concentration of antibody at which 50% of the maximum signal was observed. For the ELISA and RIA protocols,

an AP–Strep 9 conjugate or ^{125}I–Strep 9, re-spectively, was used for direct determination of the amount of antibody bound. Under the same assay conditions, the avidity of Strep 9 was determined to be 3.15×10^{-8} M from the ELISA and 3.27×10^{-8} M from the RIA (Table 1). The very similar values for avidity from both protocols show that this method of determining avidity does not depend upon the label used to detect binding.

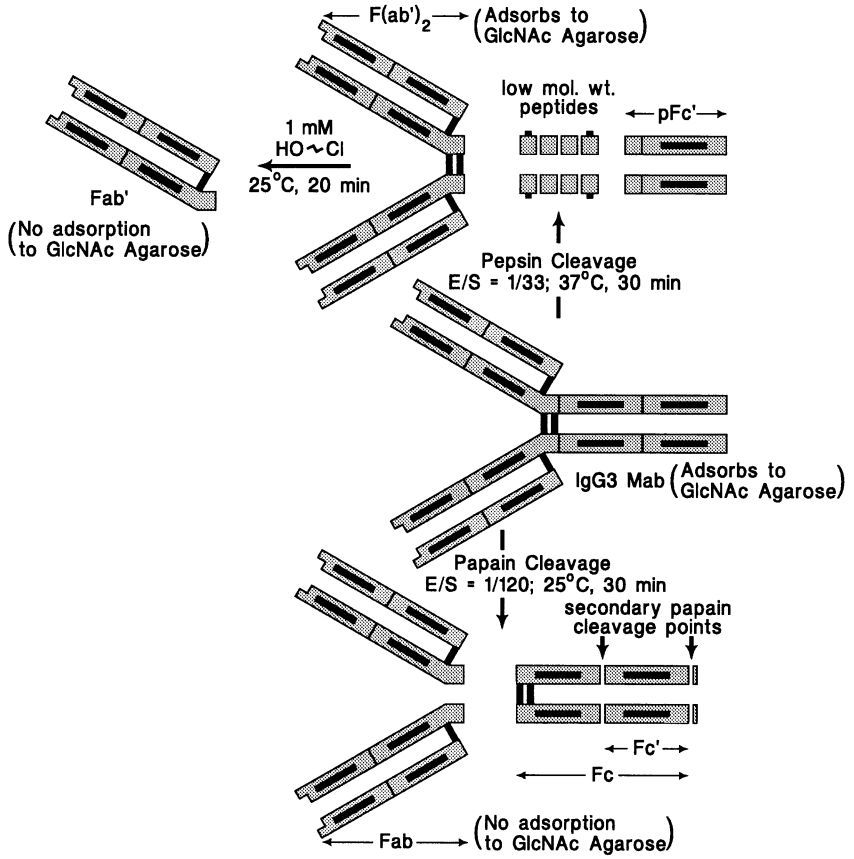

Fig. 1. Schematic representation of the antibody fragments obtained by pepsin or papain digestion.

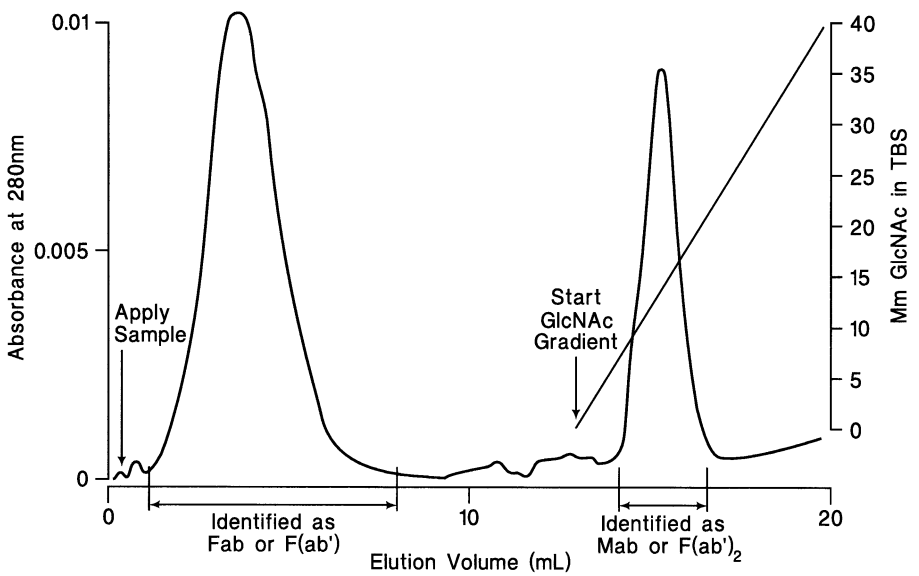

Fig. 2. Elution profile for the purification of the Strep 9 Ab, F(ab)$'_2$ and Fab using *N*-acetylglucosamine (Glc*p*NAc)–agarose affinity chromatography.

Table 1
Immunoassay data for Strep 9 mAb and Fab [a]

Antibody or fragment	K_i (M)	Incubation (h, °C)
^{125}I–Strep 9	3.27×10^{-8}	1, 37
^{125}I–Strep 9	6.1×10^{-9}	12, 25
AP–Strep 9	3.15×10^{-8}	1, 37
^{125}I–FAb	$>8 \times 10^{-7}$	1, 37
^{125}I–FAb + rat α-κ mAb (2:1)	2.3×10^{-8} [b]	1, 37

[a] In both RIA and ELISA the antibody or fragment was titrated vs. heat-killed *S. pyogenes* organisms on a microwell tray and incubated for the indicated time. In the ELISA experiments a luminescent substrate, Lumiphos 530, was used to determine bound antibody after washing.

[b] Bound/free signal was reduced over 100-fold in this experiment.

Two different incubation times were examined in the RIA: 1 h at 37 °C and overnight at room temperature. The overnight incubation yielded a value of 6.1×10^{-9} M for the avidity (Table 1). The change in the value obtained at different incubation times indicates that antibody binding had not reached equilibrium after 1 h at 37 °C.

The avidity of the Fab fragment was compared with that of the intact mAb by RIA. The ^{125}I–Fab did not bind to immobilized bacteria even at concentrations 1000 times greater than the intact ^{125}I–Strep 9. However, a modest fraction of this activity could be restored by adding a rat anti-(mouse)-kappa mAb to the ^{125}I–Fab at an optimal molar ratio of 2:1 Fab:mAb (Table 1).

A series of inhibition ELISAs was performed using a panel of oligosaccharides consisting of mono- through to hexasaccharide portions of the CWPS of GAS [12] (Fig. 3) in order to determine the fine carbohydrate-binding specificity of Strep 9. The solid-phase antigen used in these experiments was GAS that had been treated with pepsin to expose the CWPS. The order of inhibitory potency established for Strep 9 competing between the solid-phase GAS and solution-phase oligosaccharides was: CWPS > Hexa 2 (**9**) > Penta (**7**) > Tetra 2 (**6**) > Hexa 1 (**8**) > BraTri (**4**) > Tetra 1 (**5**) > Di (**2**) > Mono (1) ≫ LinTri (**3**) (Table 2).

Microcalorimetry was performed in order to determine the thermodynamic parameters of binding between Strep 9 and two of the oligosaccharide structures shown to bind the antibody well. The Tetra 1 (**5**) and Hexa 2 (**9**) (Fig. 3) both have very similar K_a values for Strep 9, approximately 10^4 M^{-1}; however, the enthalpies and entropies of binding are very different (Table 3). The binding of Tetra 1 (**5**) is dominated by enthalpy changes; in the case of the Hexa 2 (**9**) a much stronger enthalpy component is observed, although it is offset by a large opposing entropy term. This enthalpy–entropy compensation is common for carbohydrate–protein interactions [13].

A model of Strep 9 was constructed following established procedures for homology model building [14–16]. Because antibodies possess a highly conserved framework region, or immunoglobulin fold, and because a significant number of antibody crystal structures are now available, such models can be built with a reasonably high level of confidence. A composite framework based on similar antibodies was built from existing three-dimensional coordinates of antibody fragments deposited in the Brookhaven Protein Databank (BPD). The structure with the highest sequence homology to Strep 9 for both chains was the Fab fragment from the fluorescein-binding antibody 4-4-20 (Fig. 4) [17]. The hypervariable loops were added to framework regions either from existing homologous loops on 4-4-20 or from similar loops on other antibodies and proteins in the BPD. The loop with least homology to known loop sequences was CDR3 of the heavy chain, which has two prolines separated by three residues (SPAWFP). The two prolines were fixed as trans in building CDR3 in the model based on energetic considerations and because all comparable loops with a Pro-X-X-X-Pro motif found in the BPD using an alpha carbon distance searching algorithm [20] were trans proline linkages. The completed V_L and V_H domains were aligned by an RMS fit to the 4-4-20 coordinates, and the complete structure was refined by energy minimization with constraints to keep the backbone atoms in position. The resulting model is shown in Fig. 5.

A helical structure corresponding to a portion of the CWPS (24 rhamnose residues) was constructed using the glycosidic torsional angles obtained previously for a branched trisaccharide unit when complexed with Strep 9 [35]. The structure was minimized while constraining the glycosidic torsion angles; the torsion angles in the minimized structure were similar in magnitude to those used as original constraints. The oligosaccharide was then vi-

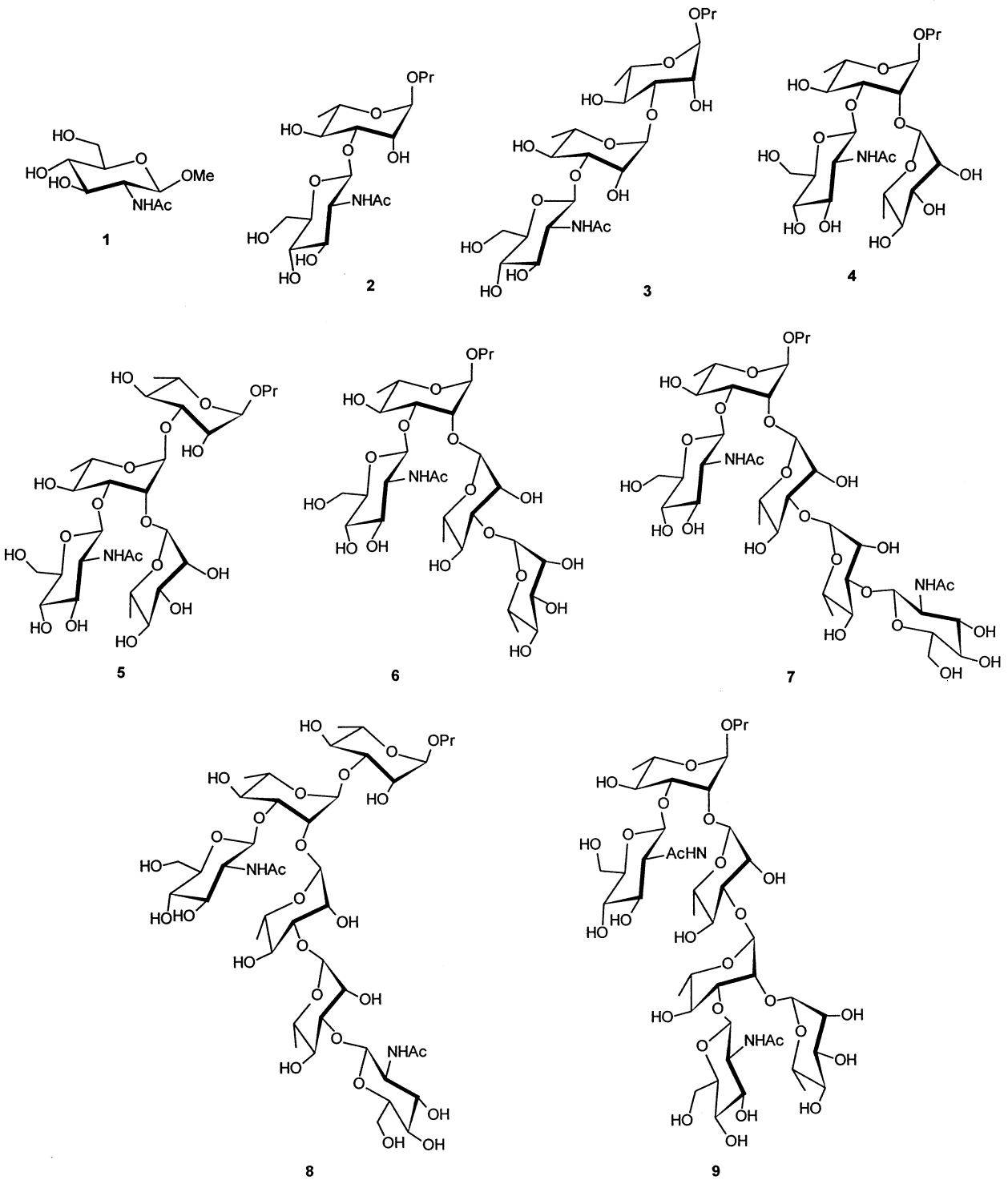

Fig. 3. Synthetic oligosaccharides corresponding to portions of the cell-wall polysaccharide of the Group A *Streptococcus* (Pr = *n*-propyl).

Table 2
Affinity constants of synthetic oligosaccharides for Strep 9

	1	2	3	4	5	6	7	8	9	CWPS
IC_{50} (μM)	413	290	[b]	135	169	50	37	61	27	10
$\Delta\Delta G$ [a] (kcal mol^{-1})	1.4	1.2	[b]	0.8	0.9	0.2	0	0.3	−0.2	−1.0

[a] $\Delta\Delta G$ determined from $\Delta\Delta G = RT \ln [I1]/[I2]$, where $[I2]$ is the concentration of the reference inhibitor, pentasaccharide **7**, $[I1]$ is the concentration of the other inhibitors both measured at 50% inhibition, $R = 1.98$ cal K^{-1} mol^{-1} and $T = 295$ K; more positive values for $\Delta\Delta G$ indicate poorer binding; differences in $\Delta\Delta G$ of less than 0.1 kcal mol^{-1} are not considered significant.
[b] 50% inhibition was never attained.

sually docked into the combining site of the Fv region, while keeping the structure of the oligosaccharide rigid. Only a few orientations for the oligosaccharide in the Strep 9 antibody combining site were possible. The two predominant orientations showed the oligosaccharide running in opposite directions. Within these two possible orientations were many possible conformations. One of these orientations is shown in Figs. 6 and 7.

3. Discussion

The different assay formats used in this investigation of Strep 9 show as much as a 1000-fold disparity between the affinity in solution and the avidity for polyvalent surface-bound antigen; Strep 9 affinity for Tetra 1 (**5**) and Hexa 2 (**9**) in solution was approximately 10^4 M^{-1}, while the K_a value for immobilized GAS was approximately 10^8 M^{-1}. Furthermore, only the bivalent antibody species, the intact mAb and F(ab)$'_2$, were able to bind to the Glc*p*NAc-agarose affinity column; the monovalent antibody species, Fab and F(ab)′, did not bind to the affinity column. These observations suggest that bivalent association between Strep 9 and the antigen is important. When monomeric oligosaccharides were used as inhibitors in the ELISA protocols or in the microcalorimetry experiments, lower values for the affinities were observed. When polyvalent GAS was the antigen, the observed affinity was high. The situation is similar for the antibody fragments. Even with the polyvalent GAS as the antigen, the monovalent antibody fragments only exhibit a low affinity value. However, the addition of rat anti-(mouse)-kappa-mAb makes a complex with the ^{125}I-Fab that can bivalently associate with the antigen. This functionally bivalent complex has an increased K_a compared with the monovalent Fab.

The inhibition ELISA data (Table 2) indicate that structures containing the branch point as represented by the BraTri (**4**) (Fig. 3) are the most potent inhibitors of Strep 9 binding to GAS. We believe this branch point to be an important feature of the epitope recognized by Strep 9, as is an extended surface since the larger structures are generally the better inhibitors (Table 2). The epitope mapping suggests that Hexa 2 (**9**), which is composed of two branched units, fully contacts the antibody since the increase in inhibitory power for the CWPS is not large. The data indicate that any benefits gained by additional contacts due to surfaces larger than a hexasaccharide might be offset by accompanying entropic costs, as is the case with a mAb directed against the O-antigen of the lipopolysaccharide of *Salmonella* serogroup B [21].

The Strep 9 antibody Fv region model binding site (Fig. 5) appears to have a distinct 'groove' character with a central pocket. The sides of the groove are flanked by CDR2 of the heavy chain and CDR1 of the light chain. Residues that form the sides of the pocket region are TYR37L, ASN96L, LEU97L,

Table 3
Thermodynamic parameters for Strep 9 binding to oligosaccharides

	Tetra 1 (**5**)	Hexa 2 (**9**)
K_a (M^{-1})	$(1.5 \pm 0.3) \times 10^4$	$(3.09 \pm 0.67) \times 10^4$
ΔH (kcal mol^{-1})	-5.8 ± 1.0	-12.02 ± 0.41
ΔG (kcal mol^{-1})	-5.70 ± 0.4	-6.14 ± 0.05
$T\Delta S$ (kcal mol^{-1})	-0.02 ± 1.0	-5.86 ± 0.41

Light chain: 81 out of 113 possible exact matches

```
        10          20          30          40          50          60
DIVMTQAAFS NPVTLGTSAS ISCRSSKSLL HSNGITYLYW YLQKPGQSPQ LLVYQMSVLA
DVVMTQTPLS LPVSLGDQAS ISCRSSQSLV HSQGNTYLRW YLQKPGQSPK VLIYKVSNRF
 *                        *---*--L1-----*-                  *-L2--

        70          80          90         100         110
SGVPDRFSSS GSGTDFALRI SRVEAEDVGV YYCAQNLELP YTFGGGTKLE IKR
SGVPDRFSGS GSGTDFTLKI SRVEAEDLGV YFCSQSTHVP WTFGGGTKLE IKR
        *       *                   -*-L3-*---
```

Heavy chain: 92 out of 114 possible exact matches

```
        10          20          30          40          50          60
-VKLLESGGG LVQPGGSMKL SCFASGFTFS NYWMNWVRQS PEKGLEWVAQ IRLKSDNYAT
EVKLDETGGG LVQPGRPMKL SCVASGFTFS DYWMNWVRQS PEKGLEWVAQ IRNKPYNYET
                          **-H1----*                    --H2-*

        70          80          90         100         110
HYAESVKGRF TISRDDSKSS VYLQMNNLRA EDIGIYYCT- SPAWFPYWGQ GTTVTV
YYSDSVKGRF TISRDDSKSS VYLQMNNLRV EDMGIYYCTG SYYGMDYWGQ GTSVTV
              *                           ---H3---
```

Fig. 4. Alignment of the sequences of Strep 9 (top) and 4-4-20 (bottom) (BPD numbering). The residues marked with hyphens indicate hypervariable loop regions and those marked with asterisks are 'invariant residues' [18,19].

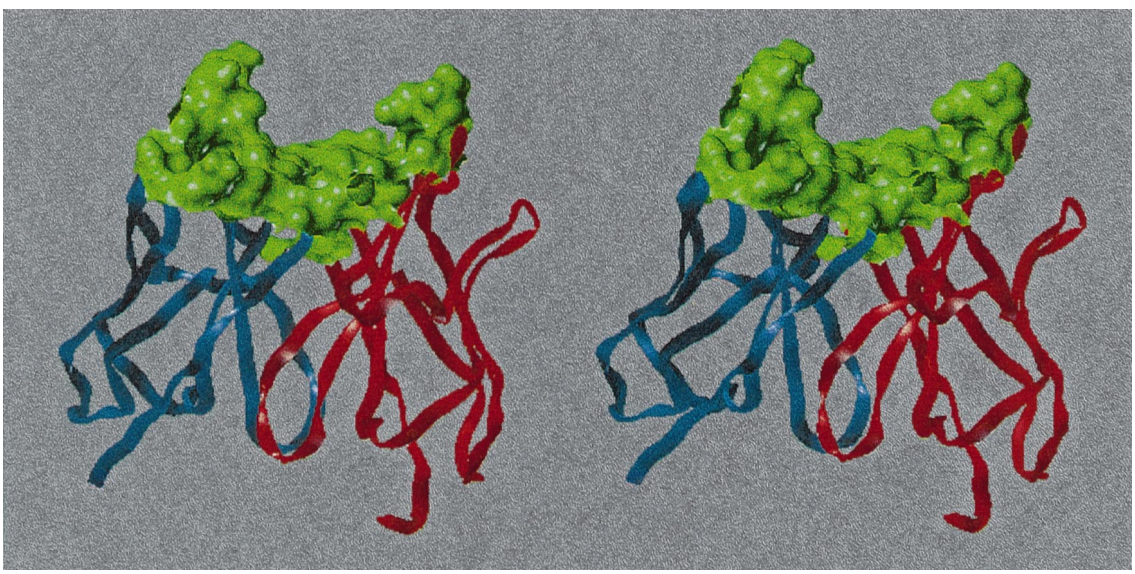

Fig. 5. Stereoview of the Fv region showing the protein backbone in a ribbon structure and the combining site in a space-filling surface. The heavy chain is shown in red and the light chain in blue.

TYR101L, TRP33H, and TRP103H. These predominantly aromatic residues are typical of antibody binding sites [22].

Docking of an oligosaccharide containing 24 rhamnose residues into the combining site gave a complex, shown in Figs. 6 and 7, in

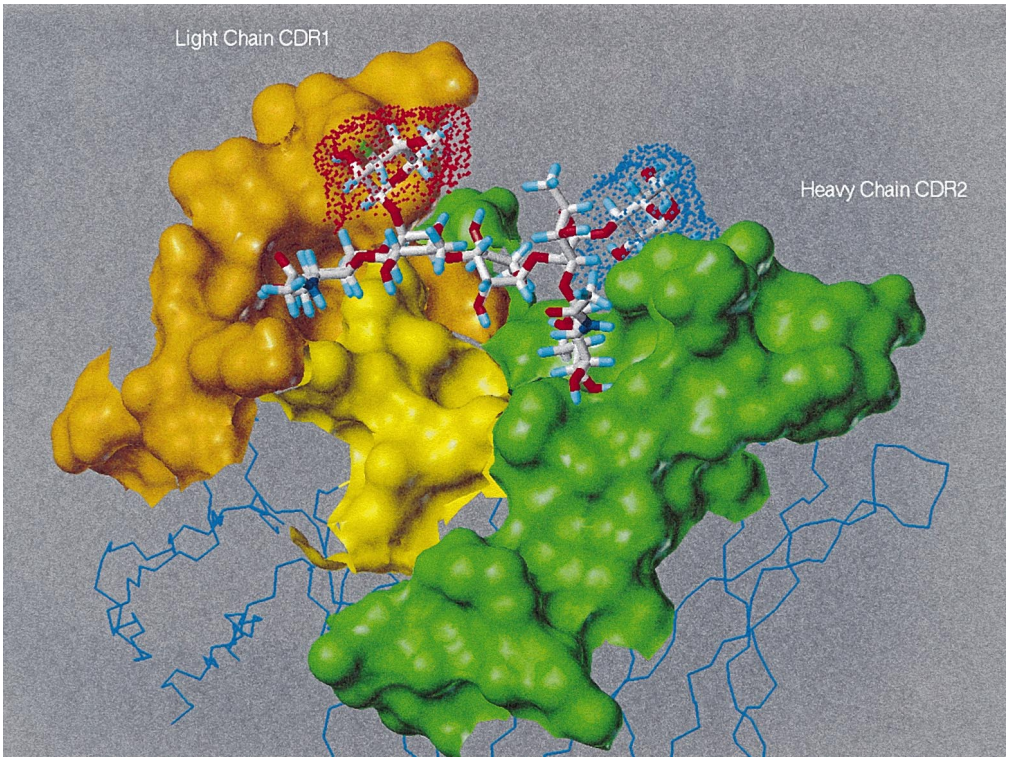

Fig. 6. Model of a Fv–oligosaccharide complex obtained by molecular modeling and docking procedures, showing the Fv region in a space-filling surface and the oligosaccharide in stick representation. The Glc*p*NAc residues are at the bottom of the site, the Rha*p* residue at a branch point is shown in a red speckled surface and the unbranched Rha*p* residue is shown with a blue speckled surface.

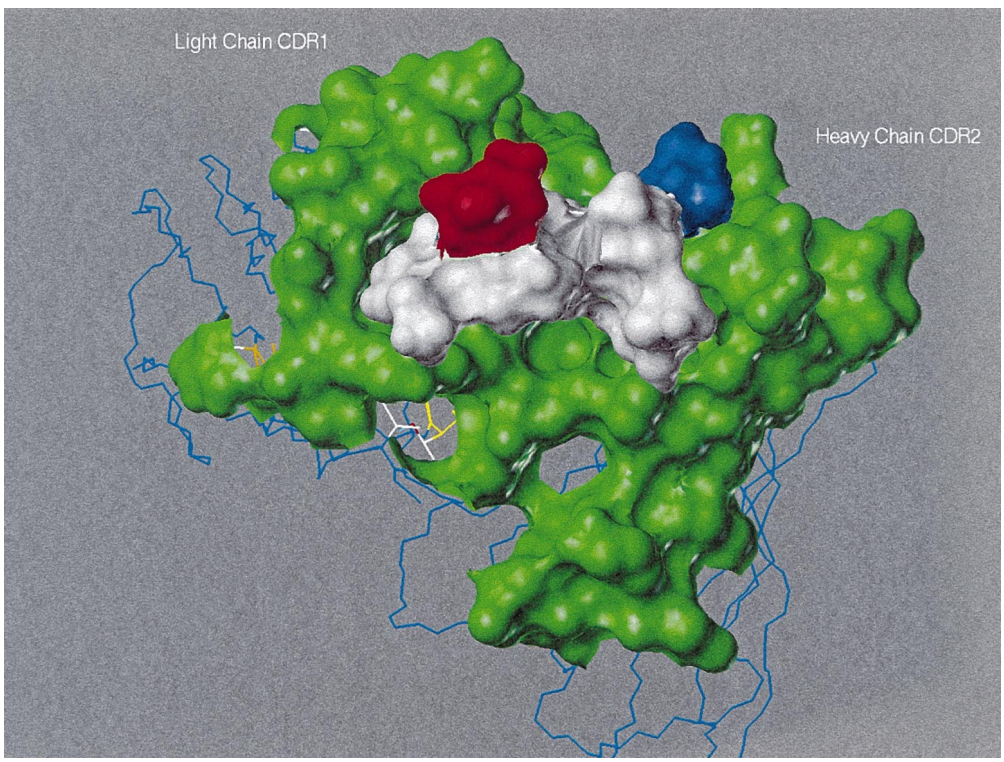

Fig. 7. Model of a Fv–oligosaccharide complex obtained by molecular modeling and docking procedures, showing, with space-filling surfaces, the complementarity between the Fv region and the oligosaccharide. The Glc*p*NAc residues are at the bottom of the site, the Rha*p* residue at a branch point is shown in red and the unbranched Rha*p* residue is shown in blue.

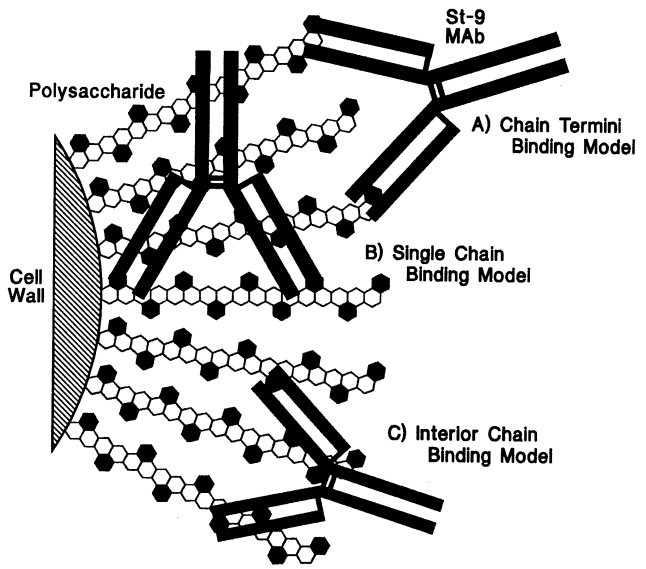

Fig. 8. Antibody–polysaccharide binding models.

which a hexasaccharide portion is accommodated in the site, with an additional unbranched rhamnose residue lying on the periphery of the site and contacting only one face of the Ab surface. The Glc*p*NAc residues from two adjacent branched trisaccharide units fit into two pockets, one in the CDR1 region of the L-chain and the other in the CDR2 region of the H-chain. There is also a deep pocket in the center of the antibody groove. This putative mode of ligand binding remains to be verified by X-ray crystallography and it is premature to comment on any ligand–protein contacts. However, it is clear that the groove-shaped binding site is capable of binding extended surfaces of the cell-wall polysaccharide.

There are three potential mechanisms for antibody binding to the CWPS on the bacterial surface [8]: (A) at two chain termini; (B) to two positions of a single chain, and (C) at interior positions of two chains (Fig. 8). Mechanism A is unlikely since the epitope mapping suggests that the optimal binding surface is provided by a hexasaccharide. Theoretical models of the polysaccharide based on molecular dynamics calculations and a chain length of 24 rhamnose residues estimate the length to be 75–80 Å [23]; thus, mechanism B is questionable. Moreover, the CWPS is only a slightly better inhibitor than Hexa 2 (**9**), again disfavoring mechanism B. Therefore, we propose that mechanism C, mAb binding to interior positions of two adjacent chains, is the most likely interaction and can best explain the high avidity of Strep 9 mAb for GAS.

Strep 9 belongs to a family of anti-GAS antibodies. This family of antibodies contains the IgM mAb, SA-3, along with antibodies (HGAC mAbs) generated by Nahm et al. [24]. The sequences of SA-3 [25] and the HGAC mAbs [26] have been previously determined; all the antibodies of this family have very similar gene usage and amino acid sequences [27]. The carbohydrate binding specificities of these mAbs are similar to those of Strep 9 [27,28]. In all cases the branched trisaccharide unit was shown to be a crucial element necessary for good inhibitory potency. Also, the more extended the carbohydrate surface, e.g., as presented by the hexasaccharide **9**, the more potent was the inhibitor.

4. Conclusions

Bivalent association between Strep 9, a murine IgG3 mAb, and its carbohydrate antigen has been shown to be important. Epitope mapping of the carbohydrate binding site revealed that the branched trisaccharide, β-D-Glc*p*NAc-(1→3)-[α-L-Rha*p*-(1→2)]-α-L-Rha*p*, and an extended surface were key components of the epitope of the Group A *Streptococcus* cell-wall polysaccharide recognized by Strep 9. Microcalorimetry experiments with a hexasaccharide showed that interaction with the Ab was favored enthalpically, but disfavored entropically, as seen with other carbohydrate–protein interactions [13]. Molecular modeling of the Fv region of the Ab based on homology modeling indicated a groove character of the combining site that was capable of binding extended surfaces of the cell-wall polysaccharide. Docking of an oligosaccharide corresponding to the cell-wall polysaccharide into the combining site provided a putative model for the complex in which a heptasaccharide unit was accommodated. Within the site were two pockets that could readily accommodate two Glc*p*NAc residues on adjacent branched trisaccharide units.

5. Experimental

Materials.—Buffer chemicals were purchased from BDH, Toronto, Ont. and Sigma Chemical Co., St. Louis, MO. Polyacrylamide was purchased from Gibco. Papain, pepsin, and the Glc*p*NAc–agarose matrix (Sigma # A 2278) were purchased from Sigma. Avidchrom CM was purchased from Bioprobe. The protein A conjugates used for the detection of Strep 9 in the ELISA protocols were purchased from Pierce, Rockford, IL. The chromogens for the ELISA protocols were purchased from Sigma, and the flourescent probe, Lumiphos 530, from Lumigen, Inc. The microtiter plates used in the ELISA protocols were either flat-bottom 96 well plates from Linbro, Flow Laboratories, Missisauga, Ont. or from Corning, Corning, NY. The microtiter plates used in the RIA and chemiluminescent protocols were μ-bottom PVC 96-well plates from Dynatech (# 001-010-2401). The plate washer used was an EL 403 autowasher, Bio-Tek, Winooski, VT, and the plate readers used were an EL 312e biokinetics reader, or a Titertek Multiscan MC, Bio-Tek, Winooski, VT. The UV spectrometer used was a Beckman DU70. An LKB scintillation counter was used. A fast-protein liquid chromatography (FPLC) system from Pharmacia was used. Gels were run on 20 cm × 20 cm × 1.5 mm Gibco slab gels.

The ^{125}I–Strep 9 and ^{125}I–Fab were prepared in house and were found to have 1.54 and 1.45 μCi/μg specific activity, respectively. The ^{125}I labeling reagents were purchased from Amersham. A Strep 9-alkaline phosphatase conjugate (AP–Strep 9) was prepared by reaction of Strep 9 with a succinimidyl-4-(*p*-maleimidophenyl)butyrate (Sigma)-modified calf intestinal alkaline phosphatase (Sigma), followed by purification on a Sephacryl S-300 column. A rat anti-kappa monoclonal Ab was used for cross-linking Fab fragments to demonstrate enhanced avidity.

The GAS samples used were grown on defibrosed horse blood and were heat-killed and treated with pepsin to expose the CWPS [29].

Generation and purification of the Strep 9 mAb.—Balb/c mice were immunized with heat-killed pepsin treated GAS [29], as described previously [28]. The ascites fluid was also generated in Balb/c mice. An *N*-acetylglucosamine (Glc*p*NAc)–agarose matrix was used for the direct purification of Strep 9 mAb from ascites. The clarified ascites was dilapidated, and buffered to pH 7.5 in TBS. The mixture was then applied to a 1.0 cm (i.d.) × 3.0 cm column of Glc*p*NAc–agarose, previously equilibrated with TBS, in a total volume of 2.2 mL. After addition of the ascites mixture, the column was thoroughly washed with TBS at a flow rate of 0.5 mL min^{-1} to remove non-adsorbed proteins. Strep 9 was then eluted with 50 mM Glc*p*NAc in TBS. The fractions containing protein (as determined by the absorbance at 280 nm) were pooled and dialyzed extensively against TBS. The final yield was approximately 3.5 mg of Strep 9 mAb/mL of ascites fluid.

Enzymatic cleavage.—The Fab was prepared by papain digestion with reaction conditions optimized for maximal disappearance of the heavy chain and minimal formation of low-molecular-weight peptides when the reaction was followed on SDS gels. The papain digestion was performed in 20 mM Tris–NaCl, pH 7.5, with 0.8 mM DTT and no EDTA. The enzyme–substrate ratio used was 0.9%. The digestion mixture was incubated for 15–20 min at 25 °C. The Fc portion was removed by precipitation when the product mixture was dialyzed against low-ionic-strength buffer, 10 mM Tris, pH 7.5. Unreacted mAb was removed on an *N*-acetylglucosamine (Glc*p*NAc)–agarose column that bound Fab much less strongly, permitting their separation.

$F(ab)'_2$ was prepared by pepsin digestion in 100 mM sodium acetate, pH 4.5, with an enzyme–substrate ratio of 1:33. The digestion mixture was incubated for 30 min at 25 °C and was followed by SDS-PAGE. Conversion of the mAb to the $F(ab)'_2$ was evidenced by an apparent mass change from 150 kDa for the mAb to 100 kDa for the $F(ab)'_2$ in 4–15% gradient gels. Isoelectric focusing indicated a pI for the $F(ab)'_2$ that was approximately 1.5 units more basic (~ 8.5) than that of the parent mAb (~ 7.0). Therefore, it was separated from unreacted mAb by cation-exchange chromatography with an NaCl gradient elu-

tion. Optimum resolution between $F(ab)'_2$ and mAb was obtained by running a shallow (approximately 10 column volumes) linear gradient of 0–250 mM NaCl across an avidchrom CM column equilibrated with 10 mM sodium acetate, pH 5.5. The $F(ab)'_2$ eluted as a single, symmetrical peak centered at 75 mM NaCl, while the mAb eluted later in the gradient at 180 mM NaCl.

F(ab)′ was prepared by reduction of 0.4 mg mL^{-1} $F(ab)'_2$ with 1 mM 2-mercaptoethylamine for 25 min at 25 °C in 20 mM Tris–HCl–0.5 M NaCl, pH 7.5 buffer. The reaction was quenched with iodoacetic acid at a final concentration of 25 mM. The conversion of $F(ab)'_2$ to F(ab)′ was confirmed by the behavior on non-reducing SDS gradient gels, and a reduction of the radius, as observed on a FPLC system equipped with a Pharmacia Superpose 12 size exclusion column.

ELISA and RIA for avidity and affinity measurements.—Microtiter plates were coated by adding 50 μL/well of GAS diluted to 10^7 organisms/mL in 0.05 M carbonate buffer at pH 9.6. The plates were left to dry overnight in a laminar flow hood at room temperature (rt) and were blocked with 150 μL/well of 1% BSA in PBS for 1 h at rt. The plates were washed three times with PBS before adding several dilutions of ^{125}I–Strep 9 for the RIA or AP-Strep 9 for the ELISA in PBS, 50 μL/well. After incubation, either 1 h at 37 °C or overnight at rt, the plates were washed three times with PBS before determining the amount of bound antibody. For RIA, the plates were cut with a hot-wire plate cutter and wells were placed in a 12×75-mm test tube for a 1 min gamma count. Wells that had not been coated with bacteria were used for background. For ELISA, Lumiphos 530 was used to determine the amount of bound antibody. The Lumiphos 530 (100 μL/well) was added and incubated at 37 °C for 30 min. Then 80 μL/well was transferred to a microtiter plate, which was read on a luminometer at 2-s integration time/well. The signals obtained, either counts/min or relative light units, were plotted against the antibody concentrations used. The results were correlated with a four-parameter logistics model that provided a good fit for the assay data and a direct estimate of avidity, i.e., the concentration of antibody that produced 50% of the maximum observed signal.

Competitive ELISA for epitope mapping

Preliminary set-up for inhibition assays versus GAS. The GAS was diluted in 0.05 M carbonate buffer at pH 9.8 to concentrations of 10^9, 10^8, and 10^7 organisms/mL, added to the microtiter plate at 50 μL/well and left to dry overnight in a laminar-flow hood. All plates were blocked with 1% BSA in PBS, 200 μL/well for 1 h at 37 °C and then washed three times with TBS. Serial dilutions of the Strep 9 antibody ranging from 100 to 0.1 μg mL^{-1} (dilution factor of $\sqrt{10}$) were prepared in PBS with 0.1% BSA. The antibody solutions (100 μL/well) were added to the plates and incubated for 2 h at 37 °C. Plates were then washed three times with TBS. A protein-A–horseradish peroxidase (HRP) conjugate, diluted 1:2000 in 50 mM Tris–HCl buffer, pH 8.5, with 150 mM NaCl and 1% BSA, was used for the detection of antibody. The conjugate was added at 100 μL/well and incubated at rt for 1 h; the plate was washed three times with TBS and *o*-phenylenediamine (OPD) (10 mg OPD in 10 mL 0.1 M NaAc buffer, pH 6, with 10 μL of 30% H_2O_2; 100 μL/well) was added. Once the color had developed, the reaction was stopped with 1 M H_2SO_4 (50 μL/well). The plate was read at 490 nm. The combination of solid-phase antigen coating and antibody concentration that produced an absorbance of approximately 0.7–0.8 was chosen for the inhibition ELISA protocol. The combination found was 10^8 organisms/mL and 3.16 μg mL^{-1} for Strep 9.

Inhibition assays. As determined in the preliminary set-up, bacteria were coated at 10^8 organisms/mL, 50 μL/well. Wells used to determine background values were coated with 2% BSA alone. Plates were blocked with 1% BSA in PBS, 200 μL/well for 1 h at 37 °C and then washed three times with TBS.

The inhibitor dilutions were made at twice the final concentration in 0.1% BSA in PBS. The final concentration range covered by the inhibitors was 0.0316–1000 μg mL^{-1} (dilution factor was $\sqrt{10}$). The Strep 9 solution was prepared in PBS with 0.1% BSA at twice the final concentration determined in the preliminary set-up. Inhibitor solution and antibody

solution were added to the microtiter plate both at 50 μL/well. Control wells received 50 μL of antibody solution and 50 μL of 0.1% BSA in PBS. The plates were incubated overnight at rt and were then washed three times with TBS. The plates were detected as in the preliminary set-up.

Microcalorimetry.—The thermodynamics of the binding of oligosaccharides by antibody was determined by titration microcalorimetry using an OMEGA titration microcalorimeter [30] from MicroCal, Inc. (Northampton, MA). Samples of approximately 50 μM antibody in 50 mM Tris–150 mM NaCl, pH 8.0, were titrated with an approximately 2 mM solution of oligosaccharide in the same buffer, at 25 °C. The ligand was injected into 20 portions of 5.0 μL, each with stirring at 400 rpm. The instrument was calibrated by standard heat pulses. Baseline determination and integration of the recorded thermograms were carried out using the manufacturer's ORIGIN* software (MicroCal, Inc.), and the binding isotherms were analyzed as described previously [21].

Molecular modeling of the Strep 9 antibody.—A molecular model of the Strep 9 antibody Fv region was built from the experimentally determined sequences of its light and heavy chains, using the SYBYL Composer program (Tripos, Inc., St. Louis, MO). Composer is based on protein homology building algorithms that have been published previously [14–16]. All energy calculations used the AMBER force field as implemented in the Tripos software [31,32]. First, sequence homologies to the respective light or heavy chain domains were determined from a database subset of individual V_L and V_H domains derived from antibody fragment structures in the BPD [33]. The best ten light-chain homologs and the best six heavy-chain homologs, respectively, were selected based on sequence identities. The 3D coordinates of conserved framework regions of the respective homologs were aligned, and the correct residues were inserted for the Strep 9 sequence using an RMS fitting procedure to the averaged alpha carbon coordinates weighted toward the templates with highest homology. After completion of the framework regions, the hypervariable loop regions (i.e., CDRs) were built using backbone coordinates of protein segments selected from the entire Brookhaven database, either by the standard method in Composer [34] or by an alpha-carbon loop searching algorithm based on that described by Martin et al. [20]. After preliminary energy minimization with the backbone atoms constrained in position, the V_L and V_H domains were aligned by an RMS fit of the conserved backbone regions of the two domains to the corresponding regions in the 4-4-20 fluorescein-binding Fab fragment (Brookhaven file 4FAB; this antibody also had the highest overall sequence homology to the Strep 9 Fv domain (Fig. 3)). After manual adjustments of close contacts, the structure was further refined by steepest descent energy minimization with gradual relaxing of side chain and loop residue constraints.

Molecular modeling of the Fv–oligosaccharide complex.—The torsion angles determined for the branched trisaccharide **4** when bound to the Strep 9 Ab [35] were used to modify the helical structure derived previously for a 24-mer [23] corresponding to a portion of the cell-wall polysaccharide. With these torsional constraints, the helix was minimized using SYBYL with the AMBER force field, modified for carbohydrates [36]. Visual docking of this oligosaccharide corresponding to the cell-wall polysaccharide into the combining site of Strep 9 was performed.

Acknowledgements

We thank the Heart and Stroke Foundation of BC and the Yukon for financial support. We are also grateful to A. Webb and D.R. Bundle for performing the microcalorimetry experiments.

References

[1] S.E. Read, J.B. Zabriskie (Eds.), *Streptococcal Diseases and the Immune Response*, Academic Press, New York, 1980.

[2] A.L. Bisno, in G.L. Mandell, R.G. Douglas, J.E. Bennett (Eds.), *Nonsuppurative Poststreptococcal Sequelae: Rheumatic Fever and Glomerulonephritis in Principles and Practice of Infectious Diseases*, 2nd ed., Wiley, New York, 1985, pp. 1133–1142.

[3] J.B. Zabriskie, *Circulation*, 71 (1985) 1077–1086.
[4] I. Goldstein, B. Halpern, L. Robert, *Nature* (*London*), 213 (1967) 44–47.
[5] I. Goldstein, P. Rebeyrotte, J. Parlebas, B. Halpern, *Nature* (*London*), 219 (1968) 866–868.
[6] I. Goldstein, L. Scebat, J. Renais, P. Hadinsky, J. Dutartre, *Isr. J. Med. Sci.*, 19 (1983) 483–490.
[7] E.M. Ayoub, S.T. Shulman, in S.E. Read, J.B. Zabriskie (Eds.), *Streptococcal Diseases and the Immune Response*, Academic Press, New York, 1980, pp. 649–659.
[8] D.G. Braun, *Microbiol. Immunol.*, 27 (1983) 823–836.
[9] J.E. Coligan, T.J. Kindt, R.M. Krause, *Immunochemistry*, 15 (1978) 755–760.
[10] D.H. Huang, N.R. Krishna, D.G. Pritchard, *Carbohydr. Res.*, 155 (1986) 193–199.
[11] E. Lamoyi, *Methods Enzymol.*, 121 (1986) 652–663.
[12] F.-I. Auzanneau, F. Forooghian, B.M. Pinto, *Carbohydr. Res.*, 291 (1996) 21–41 and refs cited therein.
[13] E.J. Toone, *Curr. Opin. Struct. Biol.*, 4 (1994) 719–728.
[14] T.L. Blundell, D. Carney, S. Gardner, F. Hayes, B. Howlin, T. Hubbard, J. Overington, D.A. Singh, B.L. Sibanda, M. Sutcliffe, *Eur. J. Biochem.*, 172 (1988) 513–520.
[15] M.J. Sutcliffe, I. Haneef, D.P. Carney, T.L. Blundell, *Protein Eng.*, 1 (1987) 377–384.
[16] M.J. Sutcliffe, F.R.F. Hayes, T.L. Blundell, *Protein Eng.*, 1 (1987) 385–392.
[17] J.N. Herron, X. He, M.L. Mason, E.W. Voss, A.B. Edmundson, *Proteins*, 5 (1989) 271–280.
[18] C. Chotia, A.M. Lesk, *J. Mol. Biol.*, 196 (1987) 901–917.
[19] C. Chotia, A.M. Lesk, A. Tramontano, M. Levitt, S.J. Smith-Gill, G. Air, S. Sheriff, E.A. Padlan, D. Davies, W.R. Tulip, *Nature*, 342 (1989) 877–883.
[20] A.C.R. Martin, J.C. Cheetham, A.R. Rees, *Proc. Nat. Acad. Sci. USA*, 86 (1989) 9268–9272.
[21] B.W. Sigurskjold, E. Altman, D.R. Bundle, *Eur. J. Biochem.*, 197 (1991) 239–246.
[22] E.A. Padlan, *Proteins*: *Stuct. Funct. Genet.*, 7 (1990) 112–214.
[23] U.C. Kreis, V. Varma, B.M. Pinto, *Int. J. Biol. Macromol.*, 17 (1995) 117–130.
[24] M.H. Nahm, B.L. Clevinger, J.M. Davie, *J. Immunol.*, 129 (1982) 1513–1518.
[25] D.C. Watson, M. Yaguchi, B. Sinnott, D.R. Bundle, N.M. Young, unpublished data.
[26] N.J. Phillips, J.M. Davie, *J. Immunol.*, 145 (1990) 915–924.
[27] S.L. Harris, L. Craig, J.S. Mehroke, M. Rashed, M.B. Zwick, K. Kenar, E.J. Toone, N. Greenspan, F.-I. Auzanneau, J.-R. Marino-Albernas, B.M. Pinto, J.K. Scott, *Proc. Natl. Acad. Sci. USA*, 94 (1997) 2454–2459.
[28] K.B. Reimer, M.A.J. Gidney, D.R. Bundle, B.M. Pinto, *Carbohydr. Res.*, 232 (1992) 131–142.
[29] R.M. Krause, *Adv. Immunol.*, 12 (1970) 1–56.
[30] T. Wiseman, S. Williston, J.F. Brandts, L.-N. Liu, *Anal. Biochem.*, 179 (1989) 131–137.
[31] S.J. Weiner, P.A. Kollman, D.A. Case, U.C. Singh, C. Ghio, G. Alagona, S. Profeta Jr., P. Weiner, *J. Am. Chem. Soc.*, 106 (1984) 765–784.
[32] S.J. Weiner, P.A. Kollman, D.T. Nguyen, D.A. Case, *J. Comp. Chem.*, 7 (1986) 230–252.
[33] F.C. Bernstein, T.F. Koetzle, G.J.B. Williams, E.F. Meyer Jr., M.D. Brice, J.R. Rodgers, O. Kennard, T. Shimanouchi, M. Tasumi, *J. Mol. Biol.*, 112 (1977) 535–542.
[34] T.A. Jones, S. Thirup, *EMBO J.*, 5 (1986) 819–822.
[35] T. Weimar, S.L. Harris, J.B. Pitner, K. Bock, B.M. Pinto, *Biochemistry*, 34 (1995) 13672–13681.
[36] S.W. Homans, *Biochemistry*, 29 (1990) 9110–9118.